Ocean Remote Sensing with Airborne K.-Band Scatterometer

S. V. Nghiem, F'. K. Li, S. H. Lou, and G. Neumann
Jet Propulsion Laboratory
California Institute of Technology
Pasadena, California 91109

Abstract - An airborne Ku-band scatterometer (NUSCAT) was used to measure ocean backscatters during the Surface Wave Dynamics Experiment (S WADE). The objective is to improve understanding of the relationship between ocean radar backscatter and near surface winds. BackScatter measurements are presented for Gulf-Stream boundary, low wind, and large wave effects. Over the boundary crossings, large air-sea temperature differences are encountered and substantial changes in the radar cross section are observed. At low wind speeds, the behavior of measured radar cross sections is different from model predictions in several cases and backscatters are occasionally very low in the cross-wind direction. Large waves due to swells have little impact at moderate winds but significantly increase backscatter at light winds.

I. INTRODUCTION

Scatterometers at K.-band have been used for remote sensing of near surface ocean winds, such as SEASAT [1] operated in 1978 and NSCAT [2] to be launched in 1996. Radar returns measured by scatterometers are primarily from the scattering by water waves on the ocean surface. The retrieval of local wind vectors is based on their correlation to the radar backscatter. The accuracy of this correlation, however, is in question when a steep temperature gradient exists across a sea surface temperature front, the wind speed is low (less than 3 m/s), or swells are in the local oceanic area. In these cases, the validity of the radar scatterometry as a technique for retrieving ocean wind field needs to be investigated,

II. NUSCAT AND SWADE

NUSCAT is a scatterometer operating at the Ku-band frequency of 14 GHz designed for airborne measurements of ocean backscatters. The scatterometer has dual polarization, a peak power of 250 W for transmitted pulses, and a dynamic range capable of observing 2-50 m/s wind with incident angles 0°-600 from fright altitudes up to 10000 m. NUSCAT system is composed of an antenna subsystem. an RF subsystem. a data subsvstem. and a controller as shown in Fig. 1. The parabolic-dish antenna has a gain of 32 dB and a pencil beam of 3°. The antenna is protected by a radome and a computer-controlled gimbal is used to steer the incident angles and rotate the azimuthal angles in a full circle. A rotary joint connects the antenna to the RF subsystem from which horizontal (H) or vertical (V) polarization pulses are transmitted with repetition frequency 4-10 kHz and pulse length 15-75 μs. When the system is transmitting H or V polarization exclusively, the data subsystem can collect-simultaneously H and V polarizations.

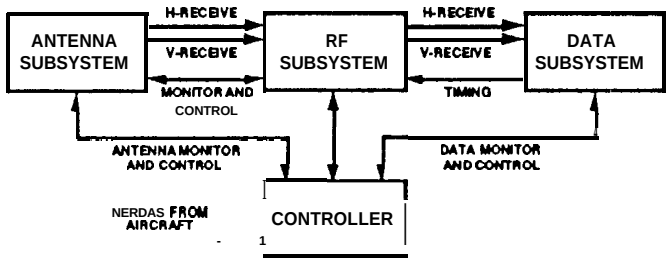

Fig.]. NUSCAT system block diagram

The Surface Wave Dynamics Experiment (SWADE) was carried out in early 1991. The experimental area is off the Wallops island as seen in the map of Fig. 2. In this oceanic area, several buoys are anchored: National Oceanographic and Atmospheric Administration (NOAA) Coastal Buoy 2 (A), Discus C (C), Discus E (E), Discus N (N), and CERC (R). The buoys collect oceanic/atmospheric data including wind vectors, air and sea temperatures, significant wave heights, and directional wave spectra. During the experiment, the Ku-band NUSCAT scatterometer, developed at the Jet Propulsion Laboratory, were flown on the Ames C-130 aircraft to obtain backscatter data from the ocean surface. The NUSCAT antenna was scanning in azimuth in 10° steps. In each step, the echoes collected over a 4-second interval were detected, averaged, and recorded before the antenna was moved to the next 10° azimuthal angle. There were a total of 10 flights from 02-27-1991 to 03-09-1991, In total, about 30 hours of data were obtained over the range of 10°-200 C in sea surface temperature, 2-14 m/s in wind speed, and 1-6 m in significant wave height.

The research described in this paper was carried out by the Jet Propulsion Laboratory, California Institute of Technology, under a contract with the National Aeronautics and Space Administration.

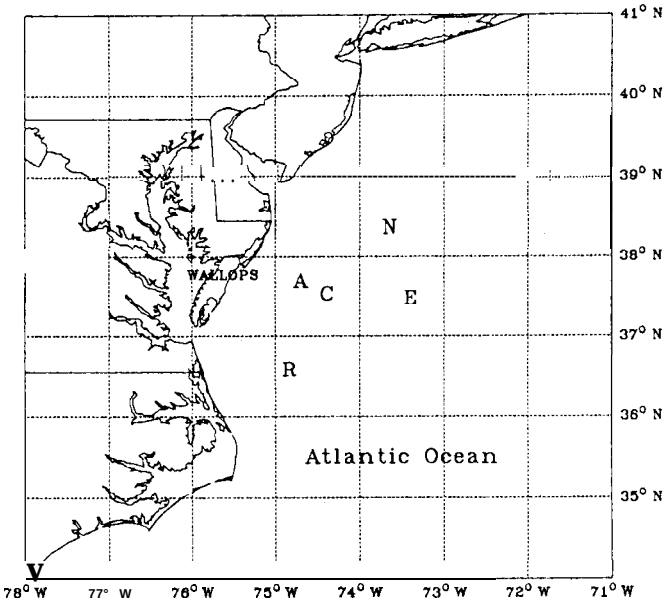

Fig.2. Experimental area of the Surface Wave Dynamics Experiment. The capital letters denotes the buoy positions: A for NOAA Coastal Buoy 2, C for Discus C, E for Discus E, N for Discus N, and R for CERC.

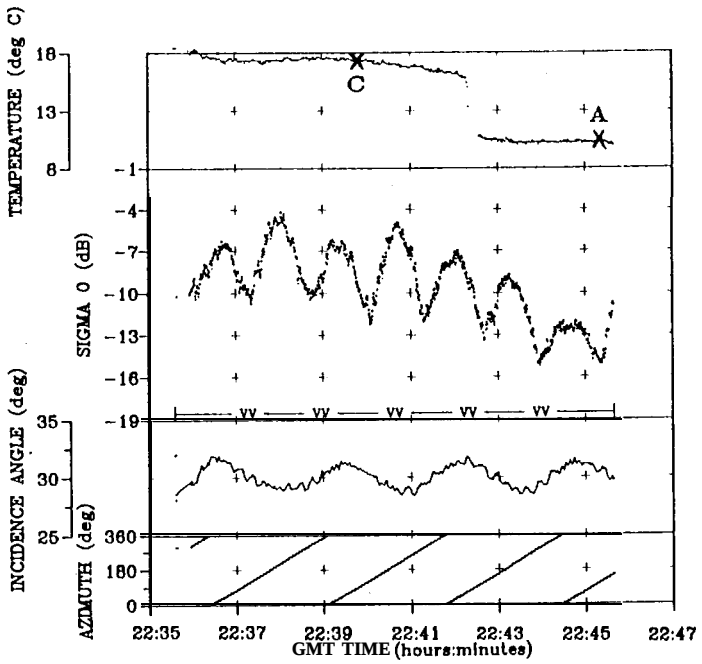

Fig.3. Sea surface temperature frontal crossing: abrupt change is seen in sea surface temperature and large decrease in backscatter was observed by NUSCAT.

III. SEA SURFACE TEMPERATURE FRONT

The boundary of the Gulf Stream was between Discus C and Discus A during NUSCAT Flight 2 on 02-28-1993. Discus C was on the warm side and Discus A was on the cold side. This abrupt change in sea surface temperature is shown in Fig. 3 together with the backscatter for vertical polarization about 30° incidence (the variation in incidence around 30° is due to the tilt of the antenna axis and fluctuations in aircraft motion angles). The corresponding decrease in backscatter observed by NUSCAT from the warm to the cold side of the sea surface temperature front is more than 5 dB in the down-wind direction as seen in Fig. 3. A factor contributing to this decrease in backscatter is the reduction by 5 m/s in neutral wind speed (U_N) from the warm to the cold side where the wind speed was 8.8 m/s at 19.5 m, converted from buoy data by using Large and Pond's formulation [3].

We compare the observed decrease in backscatter across the sea surface temperature front with that predicted by using SASS-2 model [4,5], which is an empirical model function relating backscatter to neutral winds. The comparison between observed and predicted results are shown on the plot in Fig. 4. The horizontal axis of the plot is the difference in wind speed between the two sides of the front and the vertical axis is the difference in backscatter. The thick horizontal bar represents the neutral wind speed variation within 1 hour (buoy data were recorded hourly) of the NUSCAT measurements.

From the plot, one sees that the changes in observed backscatter are larger than SASS-2 predictions. Furthermore, NUSCAT data indicate that the changes in up-wind and down-wind directions are much stronger than the change in cross-wind direction while SASS-2 backscatter variations are similar in all azimuth directions. The same results are also observed from other frontal crossings during SWADE. In these cases, using SASS-2 model to relate backscatter to only neutral wind speed is inadequate and other oceanic/atmospheric parameters, such as wind stress, may be required for comparison with the backscatter changes.

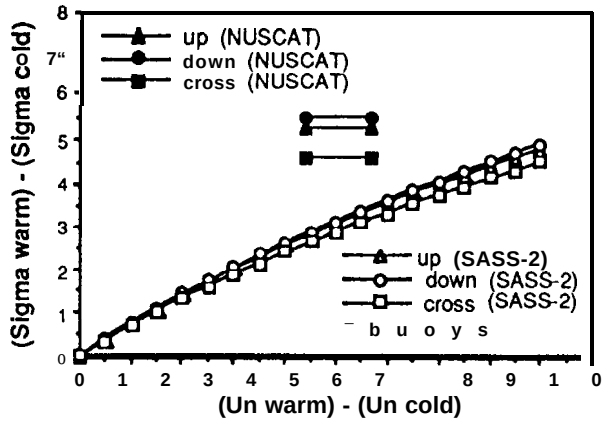

Fig.4. Comparison of NUSCAT and SASS-2 results for backscatter (V, 30°) across the sea surface temperature front,

IV. LOW WIND CASE STUDY

The wind speed encountered at the NOAA buoy was lower than 3 m/s for meet of NUSCAT Flight 3 on 1 March 1991 while the wind speed at Discus C was in the moderate range. Fig. 5 presents a case where NUSCAT flown from Discus C to the NOAA buoy. The wind speed $U_N(19.5)$ was 8.5 m/sat Discus C and dropped to 3.4 m/s at the NOAA buoy. In this case, the measured backscatter for vertical polarization at 60° incidence decreased 10 dB as seen in Fig. 5. Results for 20°, 40°, and 60° incidence are reported in Table I along with the SASS-2 model predictions. Table I shows that the NUSCAT and SASS-2 values are fairly close in the moderate wind range. For the low wind condition, however, the NUSCAT backscatter is substantially lower than the SASS-2 predictions. Thus, the increase in backscatter from low to moderate winds is larger in NUSCAT measurements as compared to the SASS-2 predictions. Another phenomenon observed at low wind is shown in Fig. 6. The wind speed at the NOAA buoy is below 3 m/s and the backscatter in the cross-wind direction markedly dropped. At up wind and down wind, the backscatter does not show this large decrease; consequently, the amplitude of the azimuth modulation in backscatter increases significantly. In the case of Fig. 6, the cross-wind backscatter is more than 15 dB lower as compared to the up-wind value. This phenomenon is observed in several low wind events and also by the University of Massachusetts C-band scatterometer flown on the same aircraft, At low wind speed, the cases studied in this paper suggest that the empirical model function needs to be modified, but scatterometry as a technique for ocean wind remote sensing still appears to be viable.

TABLE I
BACKSCATTER AT LOW AND MODERATE WINDS

	←Medium wind at buoy C→				←Low wind at buoy A→			
	θ_0	$U_N(19.5)$	NUSCAT	SASS-2	θ_0	$U_N(19.5)$	NUSCAT	SASS-2
Up	19.2°	9.4 m/s	-1.9 dB	-0.3 dB	18.7"	2.8 m/s	-11.4 dB	-4.2 dB
Down	20.0"	9.4 m/s	–1.9 dB	–1.2 dB	1 20.2°	2.8 m/s	-12.8 dB	–6.3 dB
Up	49.9"	8.8 m/s	-16.4 dB	-16.2 dB	50.5°	4.0 m/s	-28.6 dB	-22.3 dB
Down	49.5"	8.8 m/s	–16.3 dB	-16.9 dB	49.6°	4.0 m/s	–32.7 dB	-23.1 dB
Up	59.3°	8.5 m/s	–17.6 dB	-18.7 dB	59.2°	3.9 m/s	–27.5 dB	–23.2 dB
Down	60.9°	8 . 5 m/s	–18.7 dB	–20.2 dB	60.9°	3 . 9 m/s	–34.5 dB	–24.7 dB

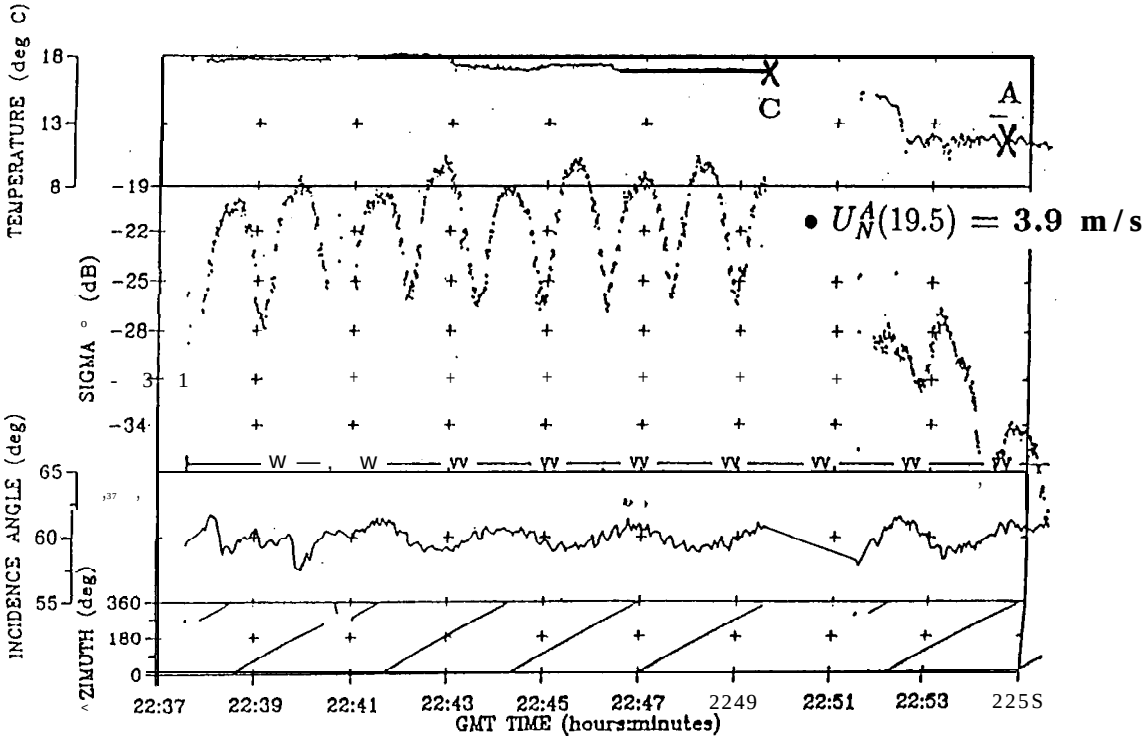

Fig.5. Measured backscatter at low wind near NOAA buoy

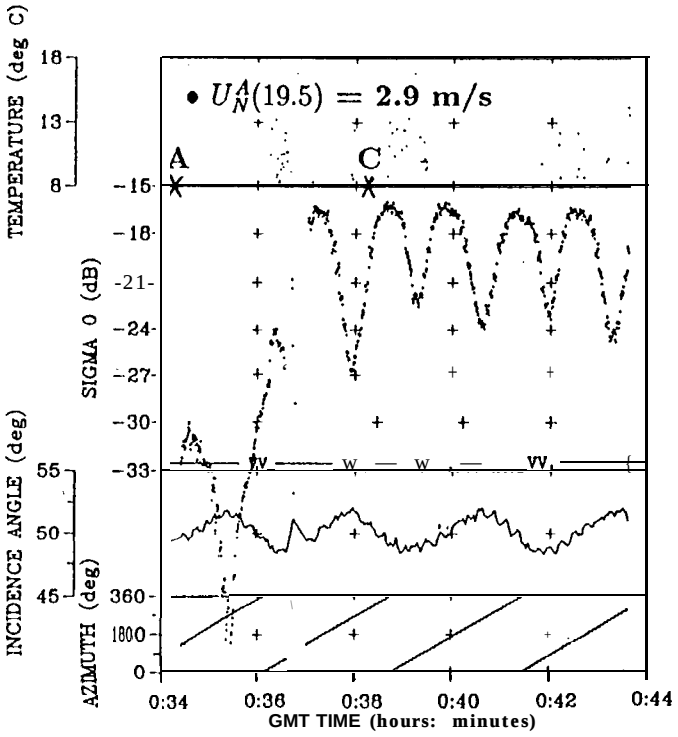

Fig.6. Marked change in cross wind backscatter at low wind

V. LARGE WAVE EFFECTS

During Flight, 5 on 03-041991, backscatter data were acquired in the presence of a swell system with large significant wave height (SWH), as high as 5.6 m. Although the wind was from the west, the wave field was dominated by a large swell from the south. The range of wind speeds corresponding to the swell cases is similar to the wind range encountered in several other flights when the significant wave heights were low. This data set presents an opportunity to compare ocean backscatters at Ku band between low and high waves.

A. Large Waves and Moderate Winds

Results for the comparison of backscatters corresponding to high and low waves at moderate wind speeds are shown in Fig. 7 with vertical polarization at *400* incidence. In this case, backscattering coefficients were all collected near Discus E where the wind speed was 12 m/s with SWH=5.5 m in the presence of swell and SWH=1.7 m for the low-wave case. Air and sea temperatures from buoy data indicate the Monin-Obukov stability lengths are negative and thus the ocean conditions for the cases under consideration are unstable. As observed from the plots in Fig, 7, there is no obvious distinction in backscatters between the cases with low and high SWH at moderate winds. In Fig. 8, the plots show an excellent agreement among NUSCAT, SASS-2, and the prediction from a model by Plant [6,7]. No significant difference is observed on the backscatter in the presence of large wave for other incident angles and horizontal polarization.

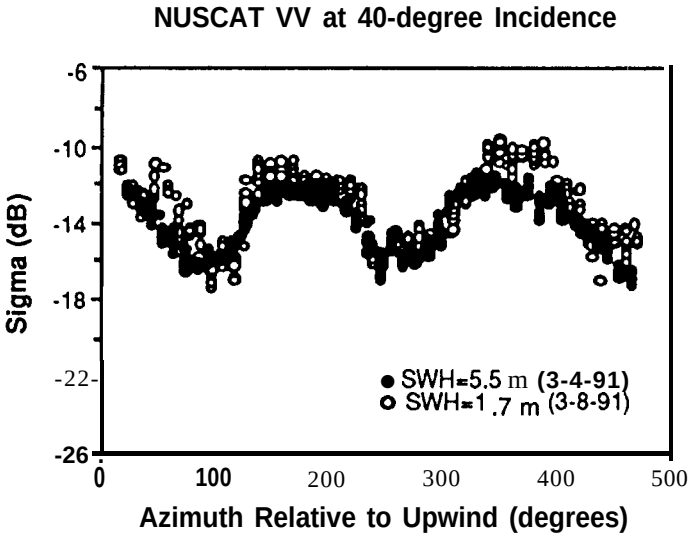

Fig.7. Comparison of NUSCAT backscatter at moderate wind speed with high and low SWH.

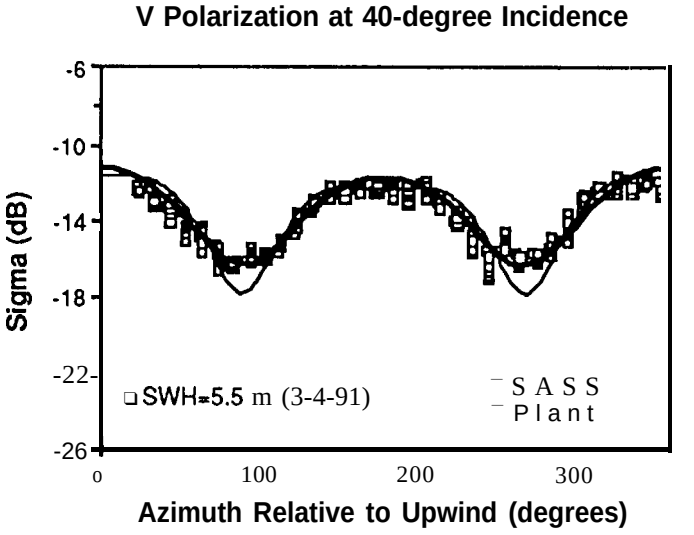

Fig.8. Comparison of NUSCAT backscatter at low SWH and moderate wind with SASS-2 and Plant's results.

B. Large Waves and Light Winds

Results at 40° incidence are plotted in Fig, 9 for measured horizontal backscatter at a light wind as functions of azimuthal angles with respect to upwind direction. For all plots of measured backscatter versus azimuth in this subsection, the "up-wind" direction is taken as the direction where the backscatter is maximized. Measured σ_{hh} for high wave are 4-5 dB higher than the corresponding backscatter for low wave in the up-wind direction as seen in Fig. 9. In Fig. 10, the data, corresponding to those for high waves shown in Fig. 9 at 40° incidence, are

compared with model values. In the model calculations, $U_N(19.5)$ = 6.6 m/s and $U_N(10)$ = 6.3 m/s are respectively used in SASS-2 and Plant's models. The measured backscatter is as much as 4 dB higher than SASS-2 and Plant's model prediction are even lower than SASS-2. Model results in these cases are more comparable to the measured backscatters for low-wave cases with similar wind speed. The analysis at smaller incident angles indicate measured backscatter for large wave is larger but the difference in backscatter is smaller. We speculate that the observed backscatter behavior in the presence of large waves is related to an increase in frictional velocity"due to wind blowing against a swell.

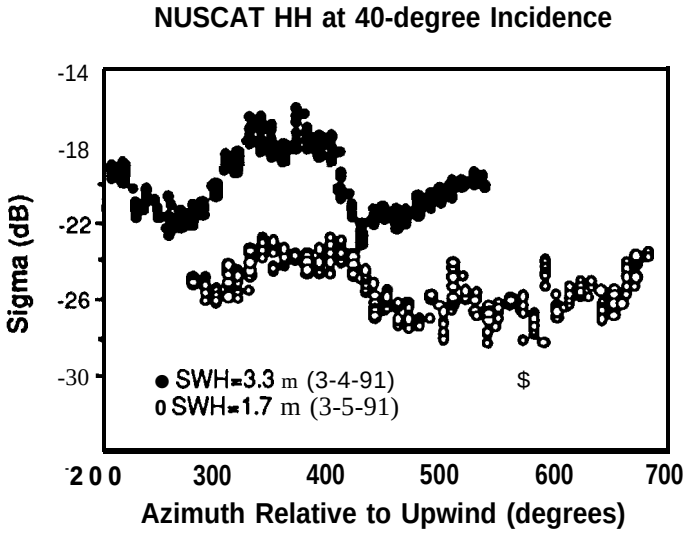

Fig.9. Comparison of NUSCAT backscatter at light wind speed with high and low SWH.

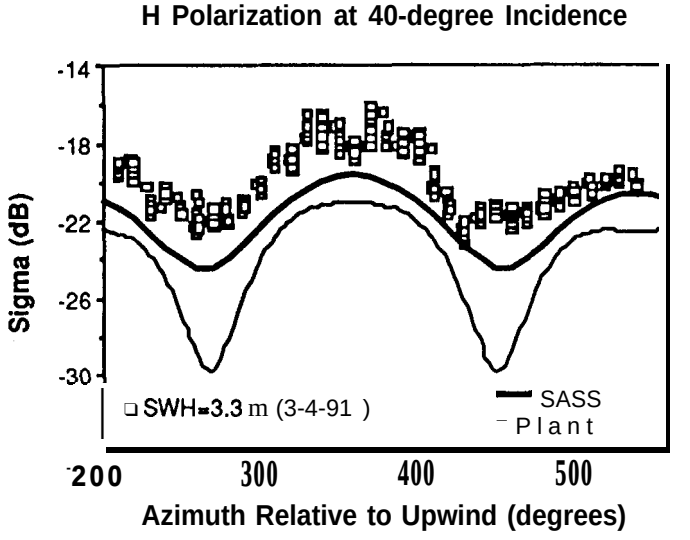

Fig.10. Comparison of NUSCAT backscatter at low SWH and light wind with SASS-2 and Plant's results.

VI. SUMMARY

Backscatter data were acquired by the NUSCAT K_u-band scatterometer during the Surface Wave Dynamics Experiment. The data are used to investigate the relationship between ocean radar backscatter and near surface winds for cases with sea surface temperature front, low wind condition, and large S WH. For the frontal crossings, variations in backscatter are larger than SASS-2 predictions based on neutral wind. At low winds, backscatter obtained by NUSCAT is smaller than SASS-2 results and very low backscatter is occasionally observed in the cross-wind direction, In the presence of large waves due to swells, the impact is negligible at moderate winds whereas the backscatter increases significantly at light winds.

ACKNOWLEDGMENT

The authors thank Drs. R. E. McIntosh and S. C. Carson for C-band data comparisons, Dr. E. J. Walsh for discussions on directional wave spectra, Drs. M. A. Donelan and W. M. Drennan for experimental observations on frictional velocities, Drs. D. Oberholtzer and K. Steele for the buoy data, and Dr. W. J. Plant for the ocean backscattering model.

REFERENCES

[1] W. L. Jones, L. C. Schroeder, D. H. Boggs, E. M. Bracalente, R. A. Brown, G. J. Dome, W. J. Pierson, and F. J. Wentz, "The SEASAT-A satellite scatterometer: the geophysical evaluation of remotely sensed wind vector over the ocean," *J. Geophys. Res.*, vol. 87, no. C5, pp. 3297-3317, 1982.

[2] F. M. Naderi, M. H. Freilich, and D. G. Long, "Spaceborne radar measurement of wind velocity over the ocean – an overview of the NSCAT scatterometer system," *Proceedings of the IEEE, vol.* 79, no. 6, pp. 850-866, 1991.

[3] W. G. Large and S. Pond, 'Open ocean momentum flux measurements in moderate to strong wind," *J. Phys. Oceanogr.*, vol. 11, 324-336, 1981.

[4] F. J. Wentz, S. Peteherych, and L. A. Thomas, "A model function for ocean radar cross sections at 14.6 GHz," *J. Geophys. Res.*, vol. 89, no. C3, pp. 3689-3704, 1984.

[5] F. J. Wentz, L. A. Mattox, and S. Peteherych, "New algorithms for microwave measurements of ocean winds: applications to SEASAT and the Special Sensor Microwave Imager," *J. Geophys. Res.*, vol. 91, no. C2, pp. 2289-2307, 1986.

[6] W. J. Plant, "A two-scale model of short wind-generated waves and scatterometry," *J. Geophys. Res.*, vol. 91, no. C9, pp. 10735-10749, 1986.

[7] W. J. Plant, Correction to "A two-scale model of short wind-generated waves and scatterometry," *J. Geophys. Res.*, vol. 93, no. C2, pp. 1347, 1988.